

Final Report for CDFA Contract Number 08-0174

Project Title: "Do Cell Wall Structures Limit *Xylella fastidiosa* (Xf) Distribution in Inoculated PD Susceptible and Resistant Grapevines?"

Principal Investigator:

John M. Labavitch, Plant Sciences Department, University of California, Davis, CA 95616

Co-PI:

Qiang Sun, Department of Biology, University of Wisconsin, Stevens Point, WI 54481

Cooperators:

L. Carl Greve, Plant Sciences Department, UC Davis

Andrew Walker, Department of Viticulture and Enology, UC Davis

Hong Lin, USDA, ARS, SJVASC, Parlier, CA 93648

Steven Lindow, Dep't. of Microbial Biology, UC Berkeley, Berkeley, CA 94720

The results reported here are for research performed between July 1, 2008 and Dec. 31, 2010.

Project objectives, activities, progress and findings (Note: The project originally proposed for a two-year research period had four objectives. However, funding was approved and allocated for only one year; thus, the objectives for the reduced support level were limited to parts of the first two that had been proposed)

Objective 1. Objective 1: Determine if the development of xylem obstructions (tyloses and pectin-rich gels) and the polysaccharide structure and integrity of pit membranes are affected by *X. fastidiosa* inoculation of grapevines transformed to express the PGIP from pear and other plant species in rootstocks and in scions. (**Note:** we did not have sufficient time to characterize PMs in healthy and inoculated pear PGIP-expressing transgenic grapevines.)

Because the data from earlier CDFA-sponsored research on the development of Pierce's Disease (PD) in grapevines have indicated that the polysaccharides in intervessel pit membranes (PMs) were an important target of Xf's cell wall polysaccharide-digesting polygalacturonase (PG) and endo- β -1,4-glucanase (EGase) (Pérez-Donoso et al., 2010) we began the use of cell wall polysaccharide-specific monoclonal antibodies (Abs) for immunohistochemical characterization of grape PM polysaccharides. Work started before this project (documented elsewhere, project 06-0225) indicated the presence of fucosylated xyloglucan (XyGs, reaction with Ab CCRC-M1) and homogalacturon pectins with a low level of methyl-esterification (low ME-HGAs, reaction with Ab JIM5)) in the intervessel PMs of PD-susceptible grape genotypes such as 'Chardonnay' and 'Riesling'. Available from our UCD colleague, Prof. A. Walker is grape germplasm that is tolerant of or relatively resistant to PD. Since the xylem system, particularly its PMs, is the pathway through which a Xf population spreads through a vine, we asked if the xylem organization and PM polysaccharide contents of Prof. Walker's PD-tolerant grape germplasm differed from that of susceptible grape genotypes.

We used five grape species/cultivars with different susceptibilities to PD for our comparison: *Vitis vinifera* cv. Chardonnay (susceptible), *V. vinifera* cv. Riesling (susceptible, but less so than 'Chardonnay'), *Muscadinia rotundifolia* (highly tolerant), 89-0908 and 89-0917 (both are selected from the cross *V. arizonica* x *vinifera* and are resistant to PD). Understanding vessel morphology is essential to elucidate possible differences in susceptibility of these grape groups, thus we have made some additional anatomical analyses of secondary xylem in our test genotypes. Our results indicate that there are major differences among these groups in the arrangement, density and diameter of vessels. In Riesling (Figs. 1A and E) and Chardonnay (Fig. 1D), vessels are relatively evenly distributed in xylem and are mostly solitary. Vessel densities also are similar in these two cultivars ($34.6/\text{mm}^2$ in Chardonnay and $30.7/\text{mm}^2$ in Riesling). However, vessel diameters in Chardonnay ($68.2\ \mu\text{m}$) are generally smaller than those in Riesling ($84.7\ \mu\text{m}$). In 89-0917 (Figs. 1B and G) vessels are not uniformly distributed in xylem tissue with a density of $42.8/\text{mm}^2$. They are usually solitary or in multiples of 3-5 cells. Solitary vessels are usually larger while most vessels in multiples are much smaller. Vessels in 89-0908 (Fig. 1F) are more or less evenly spread through the secondary xylem and usually form radial chains of 3-6 cells. Vessels have an average diameter of $66.4\ \mu\text{m}$, but individual vessels show large size differences. In *Muscadinia rotundifolia* (Figs. 1C and H) vessels usually form radial chains of 2-5 cells and individual vessel sizes ($56.5\ \mu\text{m}$ diameter, at average) vary less than in some other groups. *M. rotundifolia* vessel density is highest ($53.1/\text{mm}^2$) among the five genotypes.

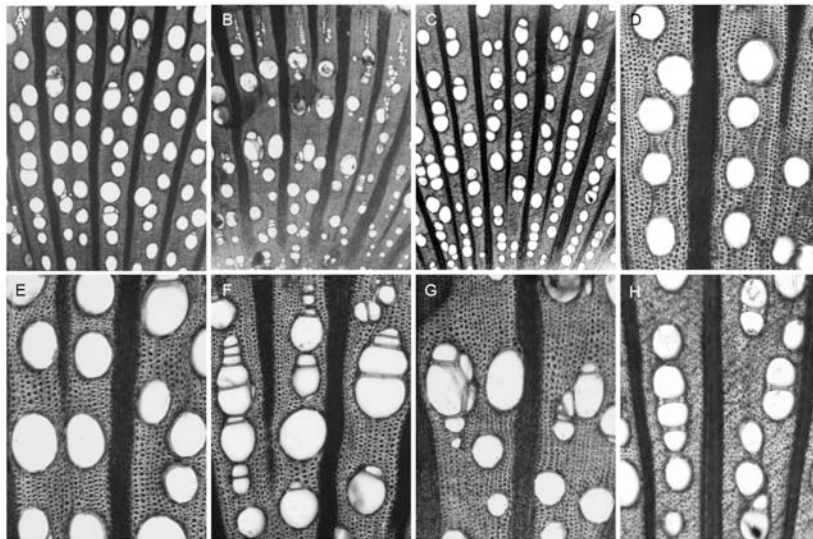


Figure 1. Differences in the distribution, arrangement and sizes of vessels among grapes of different PD susceptibilities. A and E. Riesling: Vessels are larger in diameter than other grape groups and mostly solitary, occasionally in groups of up to 3 vessels. B and G. 89-0917 grape: Vessels are usually in multiples of 3 – 5 and individual vessels differ in size. C and H. *Muscadinia rotundifolia*: Vessels of similar size are usually in radial chains of 3-5 cells. D. Chardonnay. Vessel arrangement is similar to Riesling. F. 89-0908 grape. Radial chains of 3-6 vessels are common and vessels differ in size.

Our results also indicate that the four genotypes with different PD susceptibilities all have intervessel PMs and vessel-parenchyma PMs in their vessel

lateral walls. Individual intervessel PMs are transversely elongated across the whole surface of the shared (i.e., common) wall of neighboring vessels and are arranged in a tight scalariform pattern along the vessel long axis (Fig. 2A). Vessel parenchyma PMs are round, oval or slightly transversely elongated (Fig. 2D).

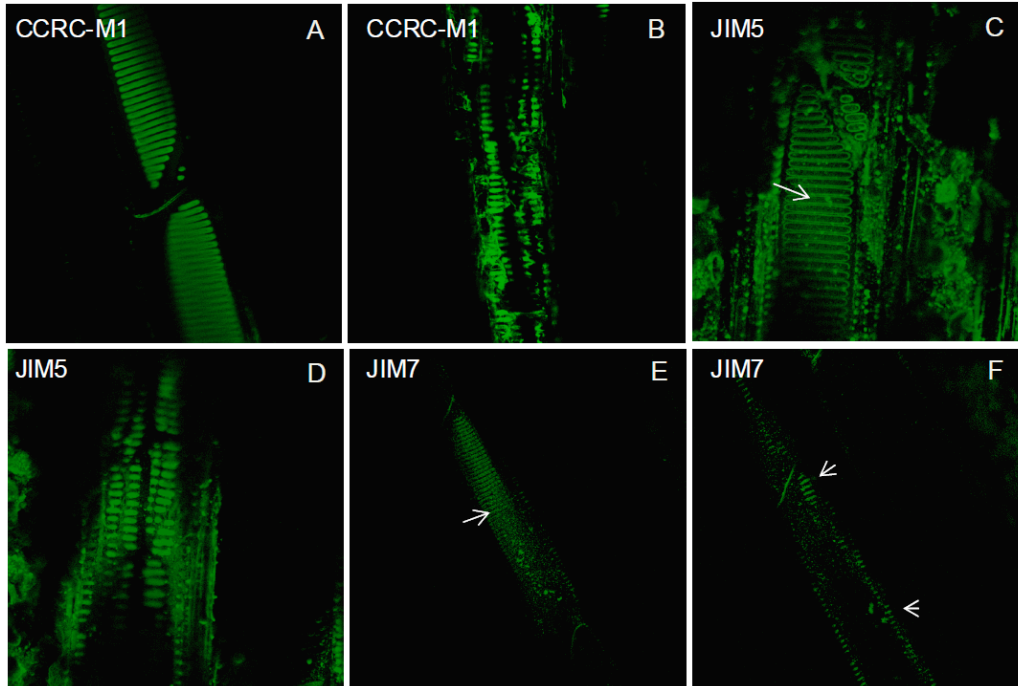


Figure 2. Cell wall compositions in intervessel PMs (A,C,E) and vessel-parenchyma PMs (B,D,F) in *Muscadinia rotundifolia*, a highly PD-tolerant grape genotype. A-B: Cell wall composition revealed by CCRC-M1, showing the presence of fucosylated XyGs in both intervessel PMs (A) and vessel-parenchyma PMs (B). C-D: Cell wall composition revealed by JIM5. Low ME-HGs are not obvious in intervessel PMs (C) but are present abundantly in vessel-parenchyma PMs (D). E-F: Cell wall composition revealed by JIM7, the Ab that recognizes highly methyl-esterified HGs (High ME-HGs). Fluorescence signal is detected from both intervessel PMs and vessel-parenchyma PMs, but is relatively weak, indicating a limited amount of High ME-HGs in both types of PMs.

The genotypes also showed differences in the polysaccharide compositions of intervessel and vessel-parenchyma PMs. In 89-0908, both intervessel PMs (Fig. 3A) and vessel-parenchyma PMs (Fig. 3B) lack fucosylated XyGs. In addition, their intervessel PMs do not have a detectable amount of low ME-HGs (Fig. 3C) or high ME-HGs (Fig. 3E). However the vessel-parenchyma PMs contain both low ME-HGs (Fig. 3D) and high ME-HGs (Fig. 3F). In *Muscadinia rotundifolia*, strong fluorescence signals were detected from both intervessel PMs (Fig. 2A) and vessel-parenchyma PMs (Fig. 2B) when incubated with CCRC-M1, thus showing fucosylated XyGs) in both types of PMs. Some high ME-HGs are also present in both types of *M. rotundifolia* PMs (Figs. 2E and 2F). Low ME-HGs occur in vessel-parenchyma PMs (Fig. 2D) but are not detected in intervessel PMs (Fig. 2C). In *V. vinifera* var. Chardonnay, fucosylated XyGs (Fig. 4A) and low ME-HGs (Fig. 4B) are abundantly present in both intervessel PMs and vessel-parenchyma PMs. High ME-HGs occur

in a large quantity in vessel-parenchyma PMs (Fig. 4D), but are undetectable in intervessel PMs (Fig. 4C).

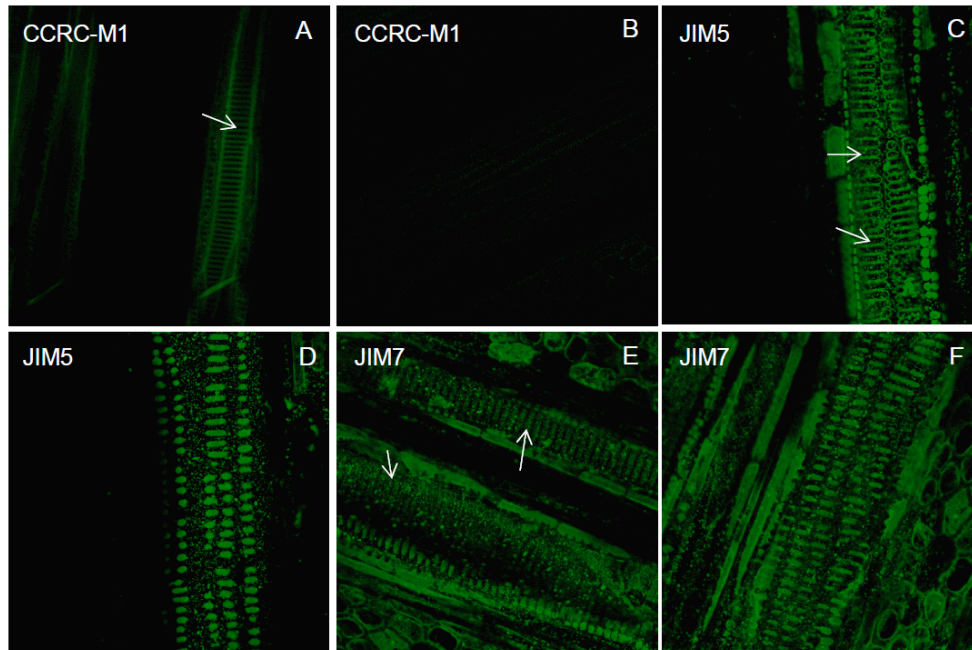


Figure 3. Cell wall compositions in intervessel pit membranes (A, C, E) and vessel-parenchyma PMs (B, D, F) in 89-0908, a PD-resistant *Vitis* genotype. A-B, No green fluorescence from intervessel PMs (A) and vessel-parenchyma PMs (B) in xylem tissue treated with CCRC-M1, indicating that fucosylated XyGs in both types of PMs are below the detectable level. C-D, PM composition revealed by JIM 5. Low Me-HGs are detected in vessel-parenchyma PMs (arrowed, D) but not in intervessel PMs (arrows, C). E-F, PM wall composition revealed by JIM7. Very weak fluorescence and relatively strong fluorescence are detected from intervessel PMs and vessel-parenchyma PMs, respectively, indicating that high Me-HGs are at a low concentration in intervessel PMs but are more concentrated in vessel-parenchyma PMs.

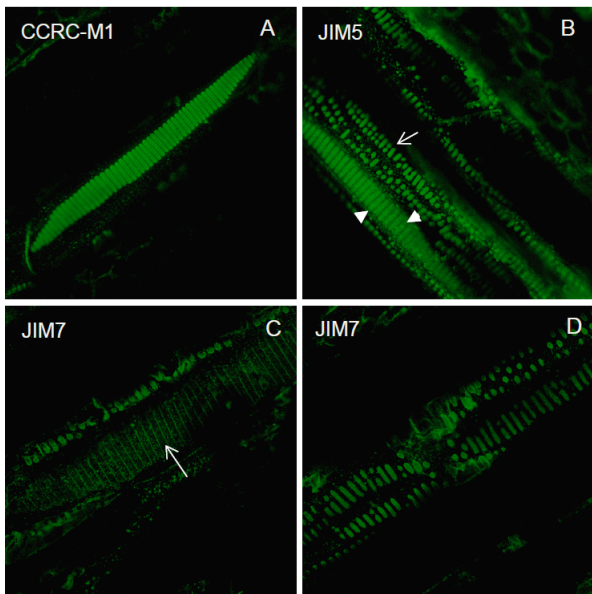


Figure 4. Cell wall compositions of intervessel PMs and vessel-parenchyma PMs in *Vitis vinifera* cv. Chardonnay, a PD-susceptible genotype. A. Intervessel PMs have strong fluorescence when incubated with CCRC-M1, indicating the abundant presence of fucosylated XyGs. B. Xylem tissue incubated with JIM5, showing that low ME-HGs are common components of both intervessel PMs (arrow head) and vessel-parenchyma PMs (arrow). C-D. Xylem tissue incubated with JIM7, the antibody that reacts with high Me-HGs. Fluorescence is below the detectable level in intervessel PMs (arrow, C) and is strong from vessel-parenchyma PMs (D), indicating that high Me-HGs are only weakly present (at most) in intervessel PMs (C) but are abundantly present in vessel-parenchyma PMs (D).

Reduced water movement capacity in PD-infected vines. The vascular system occlusions (particularly tyloses and gels) that develop rapidly in Xf-infected and otherwise stressed grapevines are particularly important factors in the infected vine's reduced water transport capacity (Pérez-Donoso et al., 2007). Therefore we used anatomical approaches to determine the extent of occlusion development in PD-susceptible Chardonnay vines. Each vine was pruned back with only two buds left at the base. Each bud then developed into a branch. When the branches were six weeks-old, one branch of each 2-branched vine was needle-inoculated with Xf at the 12th internode from the base. Separate control vines were inoculated at the corresponding internode with phosphate buffer (PB), also on one of the two branches for each control vine. Both branches of each vine (control and treatment) were limited to ca. 25 nodes in length by pruning the top. Stem internode samples were collected from both branches of each inoculated and control vine at different times post-inoculation. Included here (Figs. 5 & 6) are data from the vines at week 12 after inoculation, when severe external PD symptoms were apparent on the Xf-inoculated vines.

The vines inoculated with Xf and those inoculated with PB showed obvious differences in secondary xylem structure (Fig. 5). No vascular occlusions were observed in secondary xylem in controls, even in the internode that had been inoculated with PB (Figs. 5A, B). In vines inoculated with Xf, tylose formation in secondary xylem vessels was extensive (Fig. 5C), with other occlusions such as gels also apparent (not shown). Vascular occlusions in infected vines were not evenly distributed in vessels across the transverse sections (Figs. 5C, E). In some regions of xylem, tyloses filled most vessels (Fig. 5D), while in other regions some vessels were free of vascular tyloses (Fig. 5E). At present, the cause for this patchy occurrence of tyloses and other occlusions is not known.

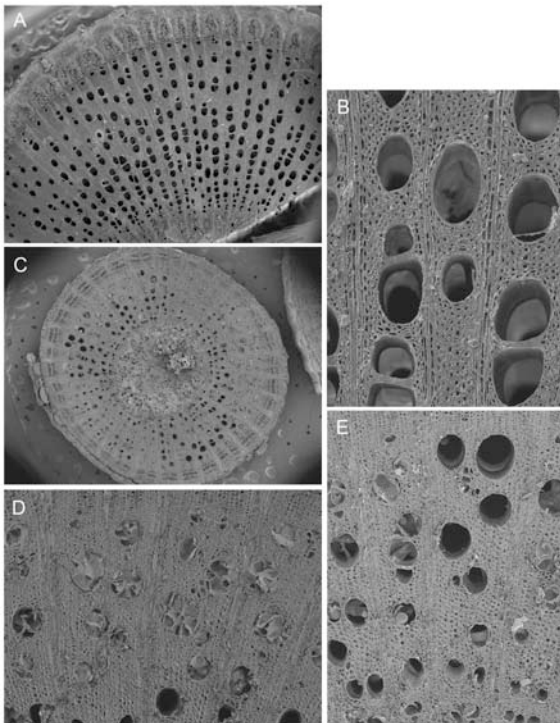


Figure 5. Xylem structure of control (A and B) and inoculated (C-E) vines. A-B: No vascular occlusions occurred in control secondary xylem vessels (A); an enlarged image shows that vessel lumens are empty (B). C: Vascular occlusions developed in secondary xylem of inoculated branches and showed uneven distribution. D: A xylem region with extensive vascular occlusions, showing most vessels blocked by tyloses. E: Xylem region with fewer tyloses and other inclusions and some open vessels.

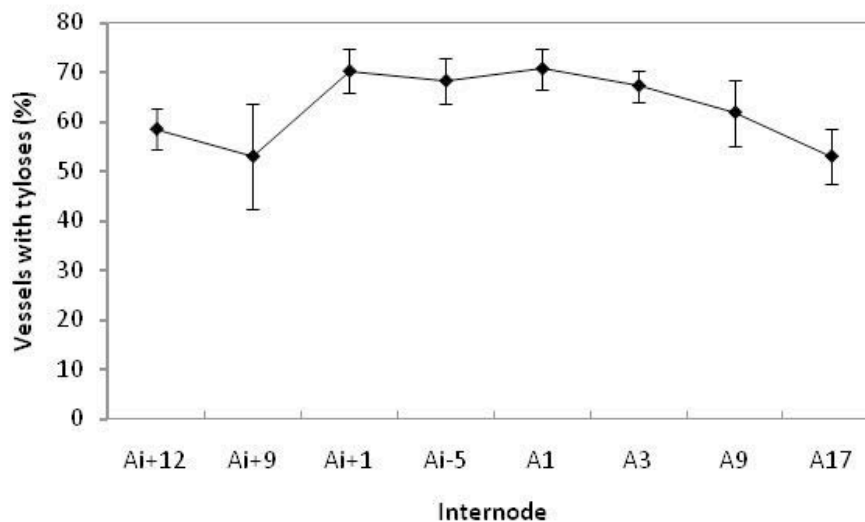


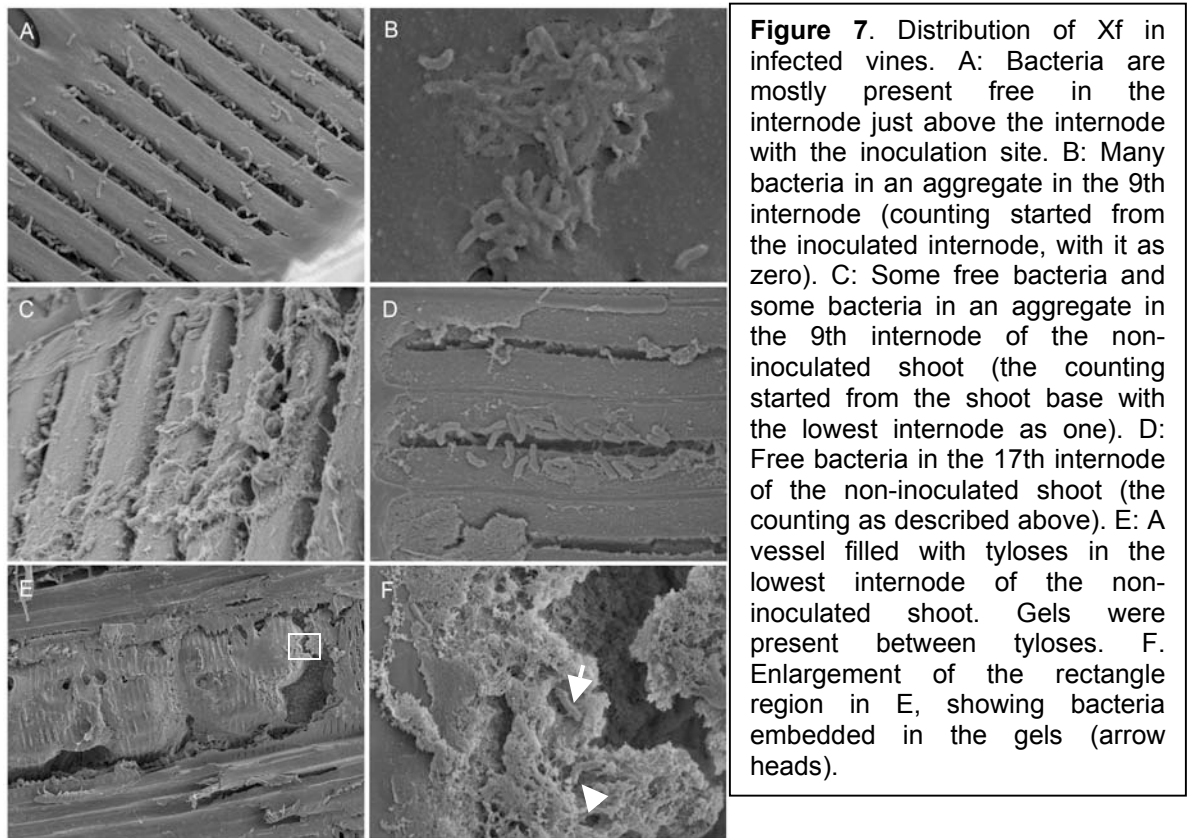
Figure 6. Quantitative comparison (based on the percentage of observed vessels that contained tyloses) of vascular occlusion occurrence observed in different internodes of the two shoots of the same vine. Recall that only one shoot of a given 2-shooted vine had been inoculated either with Xf or was a control (i.e., was PB "inoculated"). "Ai" designates the shoot of a given vine that was Xf-inoculated and "A" designates the second, untreated shoot on the same 2-shooted vine. The number following "Ai" indicates a specific internode, with the positive numbers indicating internodes above the point of inoculation and the negative numbers indicating internodes below the inoculation point. The numbers following "A" show the internode in the non-inoculated shoot, counted from its base.

Distribution of *X. fastidiosa* in inoculated 'Chardonnay' grapevines In the vines with severe external PD symptoms, Xf cells were observed in all internodes of both the inoculated and uninoculated branches of 2-shooted vines that had been directly inoculated in only one shoot (Fig. 7). This indicated that the bacteria could move both upward from the inoculation site and downward to the trunk shared by the two branches and then move upward in that uninoculated shoot.

Our observations also indicated that bacteria in the vines with severe external PD symptoms were present in very few vessels. Vessels with Xf were usually present in less than 10% and 3% of all vessels in the inoculated and non-inoculated shoots, respectively. The numbers of bacteria in the affected vessel were also larger in the internodes of inoculated shoots than in non-inoculated shoots. In no case, however, was an Xf population that was sufficiently large to completely block vessels observed, as has been suggested by earlier studies. Since Xf cells were only present in few vessels in limited numbers, a direct influence of bacterial population presence on the water transport through the vessel system should be very limited.

Xf cells were present in vessel lumens in several different forms. Most commonly, they occurred as free individuals (Figs. 7A and D). Bacteria in this form were observed in the internodes of both inoculated and non-inoculated shoots. Aggregates of 2-6 cells in which bacteria are loosely bound together through a filamentous network were also common (Fig. 7C). Occasionally, aggregates of tens to hundreds of bacteria were observed in vessel lumens (Fig. 7B). Bacteria were also observed between loosely or compactly arranged tyloses (Figs. 7E and F). In

this case, bacteria were always embedded in gels whose origin (either tylose or bacterium) is not clear at present.



Objective 2. Determine whether there are differences in pit membrane porosity or polysaccharide structure between resistant and susceptible grapevines. To what extent are these PM characteristics and the production of tyloses and gels modified by introduction of *X. fastidiosa* to PD-resistant and -susceptible genotypes? (**Note:** We received funding from the UC Pierce's Disease Control Board [USDA, project 10-0266, Sun, PI, and Labavitch] to support work related to Objective 2 and this work is ongoing. Here we report just on our work related to the changes in PM integrity in Xf-inoculated PD susceptible 'Chardonnay' grape)

We investigated the impact of Xf on intervessel PM integrity by using PD-susceptible Chardonnay vines. Each vine was trained to two shoots with one shoot needle inoculated with Xf at the 12th internode from the shoot's base, as described earlier in this report. Control vines were inoculated with PB. Internode samples were collected from both shoots of each vine weekly after the inoculation. The data reported here are from both infected vines and control vines at Week 12 after treatment when the infected vines had shown severe PD symptoms.

Comparison of intervessel PM integrity between control vines and Xf-infected vines In secondary xylem of grapevines, pits between adjacent vessels are

horizontally elongated bordered pits which are arranged in a scalariform pattern (as in the rungs of a ladder) along the long axis of the vessel elements. For each pit, the borders of the secondary cell wall are arched over the PM, which is composed of the primary cell walls of the two adjacent vessel elements and the shared middle lamella). Only a very small portion of the PM can be seen through the slit-like opening in the secondary wall in the surface view. From the perspective of the vessel lumen, the 2° cell wall arches over the PM like a roof with the slit-like aperture serving as a "skylight" through which only a small portion of the PM surface can be seen (Fig. 8A). However, the entire PM can be clearly examined for its integrity with a scanning electron microscope (SEM) after the removal of the secondary wall borders (Fig. 8B). Figs. 8C and D compare the PM surfaces of Xf-inoculated PD-susceptible and -resistant grape germplasm.

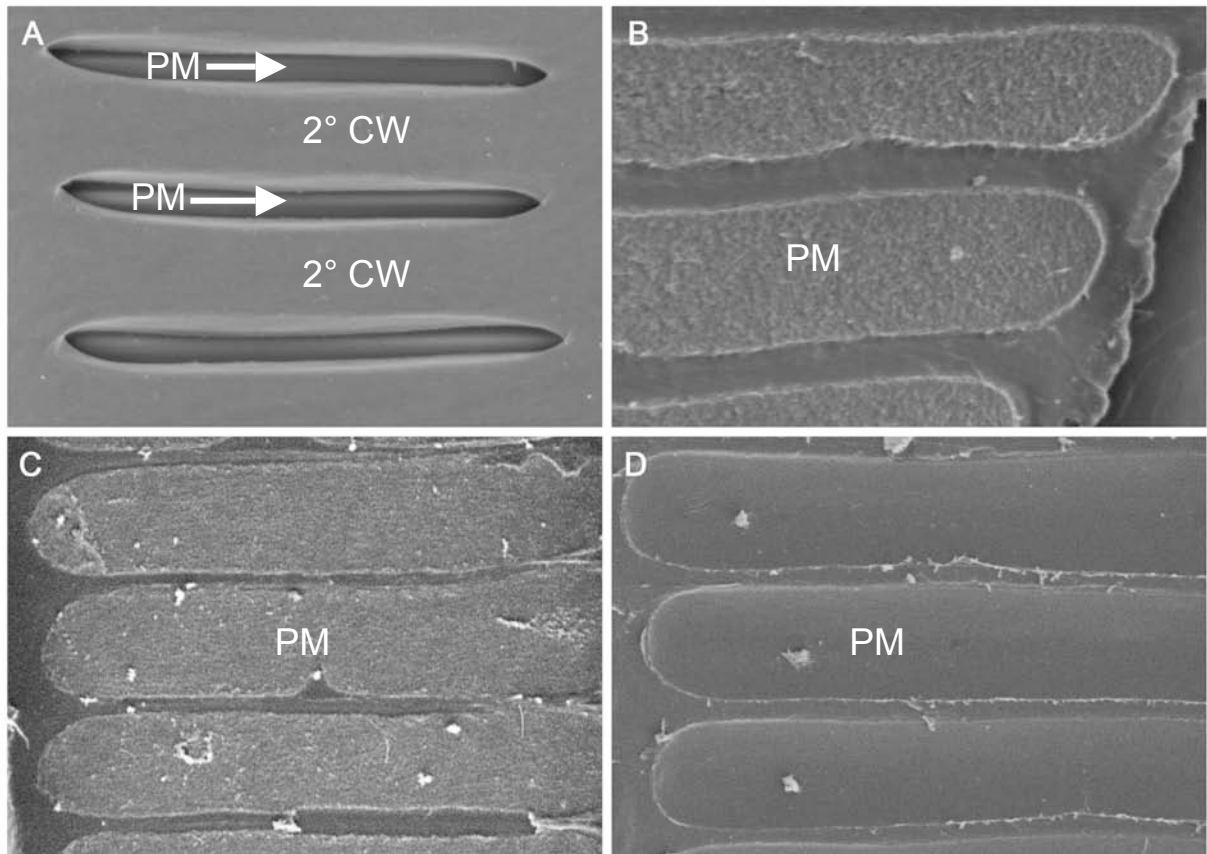


Figure 8. Scanning electron micrographs of intervessel pits and PMs in secondary xylem of a control 'Chardonnay' vine. A & B: uninoculated vines. A. Bordered pits, showing secondary cell wall borders (2° CW) and PMs viewed through narrow pit apertures. B, C, D: B. Intact PMs are exposed after the secondary cell wall borders have been peeled away. C: Exposed PMs of an Xf-inoculated 'Chardonnay' vine. The surface appears to be a bit rough, but no Xf cells are present yet. D: Exposed PMs of an Xf-inoculated, PD-resistant grape genotype.

The Xf-occupied vessels of some inoculated 'Chardonnay' vines, PM barriers are eventually degraded (Fig. 9). Our attempt to determine the progression of events in Xf's PM degradation process was based on the inoculation of several 'Chardonnay' vines and the subsequent sampling of internodes in excised shoots at

intervals so that SEM could be used to examine changes in PM integrity (Fig. 9). Of course, our identification of time-dependent stages of PM breakdown is speculative since we are not able to follow the degradation of individual PMs. Thus we must infer the timing of events based on sampling of inoculated vines at different times after their inoculation. We know that individuals in a set of inoculated vines do not develop PD over the same time course.

PM degradation usually occurred initially as small separate patches in the central region of a PM (Fig. 9A). The PM surface in these patches became rough, probably because some wall materials have been removed and the remaining wall materials are loosely arranged and extend out (toward the vessel lumen) from the PM surface. As more wall materials are removed, the rough region of the PM may expand to cover a central band region throughout most of the PM's width (Fig. 9B) and tiny pores in the PM region are visible under the loosely arranged surface wall materials. The peripheral region of the PM at this stage is intact and remains relatively smooth. The next images (Figs. 9C and D) suggest that most of the "frayed" PM surface material shown in 9B has been removed, exposing small pores in the central region of the PM. Further degradation of the PM includes the enlargement of the pores in the PM's central region and the appearance of new pores in its peripheral region (Figs. 9E and F). Some pores may be large enough for *Xf* cells to pass through. The increased porosity also weakens the PM itself and subsequently a crack along the central region of the PM throughout its width has developed (Figs. 9E and F). It seems that the two primary surfaces of a PM (i.e., the primary cell wall of each of the neighboring vessels that "shares" a given PM) are no longer tightly attached at this stage, because the separation of the two primary walls of the damaged PM is common at this stage (Fig. 9E). The highly porous PMs may be partly or completely detached from their original positions and the PM barriers between adjacent vessels may eventually disappear.

Xf cells were frequently observed inside pit chambers. They are mostly present in the central region of a PM (Fig. 10A), probably because the secondary wall borders of a pit arch over the PM, leaving spaces that are too small for *Xf* cells to accumulate in the peripheral regions of the PM. The degradation of the PMs associated with *Xf* cells occurred in the same way as described above. At the beginning, the central region of PMs is commonly rough (Fig. 10B) and has tiny pores that can be seen wherever bacteria are absent. As more wall materials have been removed from the PM, the size and number of the pores in the PM increase (Figs. 10 C and D). Further degradation of this PM will greatly reduce its integrity as well as its strength and leads to its complete or partial removal from its original site (Figs. 10 E and F). It is reasonable to assume that PMs that have been broken down to the extent shown in Figs. 9 E and F and Figs. 10 E and F no longer contribute to an effective grapevine suppression of the systemic spread of the *Xf* population.

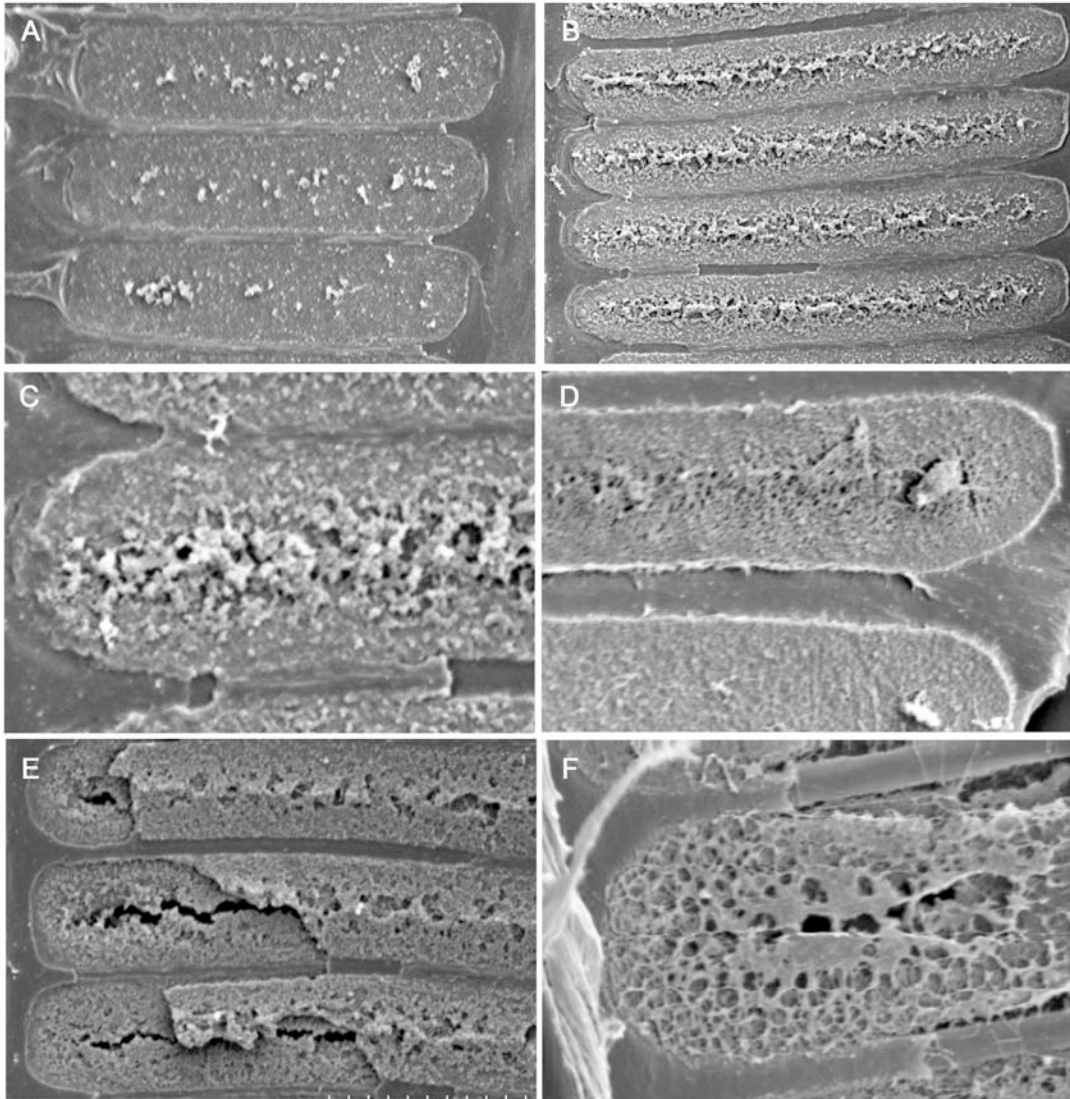


Figure 9. Scanning electron micrographs of intervessel PMs in secondary xylem of a *Xf*-infected Chardonnay vine, showing the PM degradation process. A: Few rough patchy regions with loosely arranged PM wall material. B: A central band of PM surface becomes rough with loose wall material. C: An enlargement of the rough PM surface shown in B. D: An enlargement of part of panel B showing tiny pores that have developed under the wall material. E: Two primary cell walls of each PM. The facing primary wall is highly porous and part of it is gone. The primary wall beneath forms a crack across its width. F: Large pores are present throughout the facing primary wall of the PM.

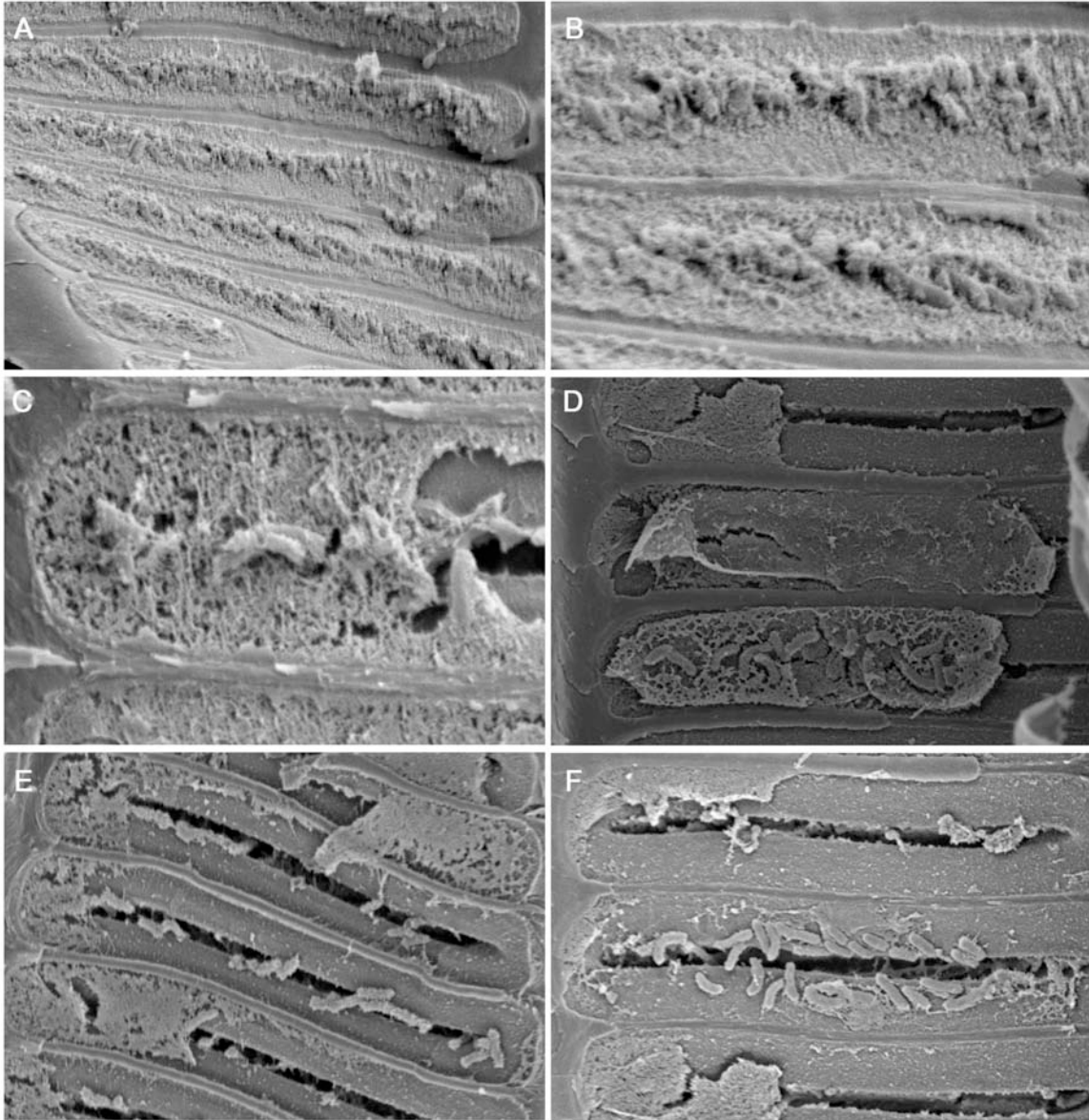


Figure 10. Scanning electron micrographs of intervessel PMs associated with Xf cells in 'Chardonnay' vines, showing the different stages of PM degradation. A. Xf cells are accumulated in the central region of each PM. B. The enlargement of part of panel A, showing tiny pores and the rough PM surface. C. Porous PM after the removal of more wall materials. D. Degradation does not occur simultaneously among different PMs. The facing primary wall has disappeared in the upper two PMs but is present and highly porous in the lowest one. E-F. PMs have partly or completely disappeared and the remaining parts of the PMs are highly porous. Clearly the opening in the PMs are sufficiently large to allow rather free passage to the Xf cells in the vicinity of the PM gaps.

Intellectual Property:

No new intellectual property will be directly developed from this work. The results reported here and in the recently completed project 06-0225 provide information that confirms our hypotheses about the roles played by *X. fastidiosa*'s EGase and PG in facilitating the pathogen's systemic spread in grapevines. We are currently working to determine if rootstock production and export of plant PG-inhibiting proteins can be used to protect vines from PD. The data that suggest a difference in the polysaccharide make-up of PMs in PD-susceptible and -tolerant grape genotypes (discussed above and in Sun et al., 2011) suggest that immunohistochemical analysis of PM polysaccharide compositions might be a useful early screen for resistant vs. susceptible grape germplasm. At present, however, more data will be required to confirm the validity of such a screen. In general, the work that we are doing is designed to provide a more detailed understanding of relatively early events in *X. fastidiosa*'s colonization of grape tissues (and probably also of other plant tissues that are infected by the bacterium). It is our belief that such information will help identify additional strategies for enhancing grape's ability to defend itself against *X. fastidiosa* without irreparably harming itself in the process.

Appropriate References:

Pérez-Donoso AG, Q Sun, MC Roper, LC Greve, B Kirkpatrick and JM Labavitch (2010) Cell wall-degrading enzymes enlarge the pore size of intervessel pit membranes in healthy and *Xylella fastidiosa*-infected grapevines. *Plant Physiology* 152:1748-1759.

Pérez-Donoso A, LC Greve, JH Walton, KA Shackel and JM Labavitch (2007) *Xylella fastidiosa* infection and ethylene exposure result in xylem and water movement disruption in grapevine shoots. *Plant Physiol.* 143:1034-1036.

Sun G, Greve LC and JM Labavitch (2011) Polysaccharide compositions of intervessel pit membranes contribute to Pierce's Disease resistance of grapevines. *Plant Physiology* 156: (in press).

The Relationship of the Potential Results from this Project and Solutions to the PD Problem in CA:

The ability of pit membranes to withstand the impacts of Xf and its cell wall-degrading enzymes and prevent the systemic spread of the pathogen appears to be a key to grapevine resistance to PD. Continuing studies based on the ideas that were explored for the first time in project 06-0225, continued with project 08-0174, and remain on-going in our team (project 10-0266). Whether this continuing work (projects 08-0171 and 10-0266) identifies additional opportunities for grapevine protection is not certain at this time.